JOURNAL OF MATERIALS SCIENCE 25 (1990) 3221–3228

An evaluation of the grain-boundary sliding contribution to creep deformation in polycrystalline alumina

A. H. CHOKSHI
Department of Applied Mechanics and Engineering Sciences, University of California, San Diego, La Jolla, California 92093-0411, USA

The occurrence of grain-boundary sliding during creep in fine grained alumina was examined by inscribing marker lines on the tensile surfaces of specimens, prior to testing in four-point bending mode. There was considerable microstructural evidence for the occurrence of grain-boundary sliding and grain rotation during creep deformation. Experimental measurements of the offsets in the marker lines at grain boundaries reveal that the grain-boundary sliding contribution to the total strain during creep deformation is 70 ± 6.2%. The extensive grain boundary sliding observed, together with the other mechanical properties, suggests that polycrystalline alumina exhibits superplastic characteristics. Several possible rate controlling mechanisms are examined critically in light of the present results and it is concluded that creep occurs either by an independent grain-boundary sliding mechanism or by an interface controlled diffusion mechanism.

1. Introduction

Ceramics and ceramic composites are being considered increasingly for structural applications at elevated temperatures. Currently, there is considerable interest in developing superplasticity in ceramics so that they may be formed easily into useful components [1–6]. It is well known that grain boundaries play an important role in the deformation and fracture of polycrystalline materials at elevated temperatures. The occurrence of grain-boundary sliding may contribute substantially to creep deformation in fine grained materials. Also, cavities may nucleate under the stress concentrations caused by grain-boundary sliding and this may lead to premature failure in some materials. Therefore, a complete understanding of the mechanical properties at elevated temperatures requires a characterization of the role of grain boundaries in both deformation and failure.

There have been many detailed studies on cavitation failure in structural ceramics [7–16]. It is generally assumed that cavity nucleation during creep deformation occurs under a stress concentration developed during grain boundary sliding [10, 11, 15, 17–20]. However, there is very little quantitative information available on the occurrence of grain-boundary sliding in structural ceramics.

Grain-boundary sliding has been examined extensively during creep deformation in polycrystalline metallic alloys, and most of the information available has been summarized in several reviews on the topic [21–24]. These studies show that the ratio of the strain due to grain-boundary sliding to the total creep strain, ξ, increases with a decrease in both the grain size and the imposed stress. Thus, for example, experiments on fine-grained superplastic alloys which deform at low flow stresses show that $\xi \gtrsim 50\%$ under optimum superplastic conditions [25]. The occurrence of grain boundary sliding in ceramics has been deduced indirectly from the formation of cavities along grain boundaries and at triple-point junctions [10, 11, 15, 17, 19, 20], the observation of strain whorls along grain boundaries by transmission electron microscopy [26] and internal friction experiments [27–29]. The occurrence of grain-boundary sliding in ceramics has also been noted directly from the offsets in bicrystals along grain boundaries [30, 31], the offsetting of triple point junctions [32], the formation of corrugated boundaries [33], the formation of boundary steps perpendicular to the specimen surface [20, 34–38] and the sharp offsets at grain boundaries in initially continuous marker lines [39–44]. However, in contrast to metallic alloys, there have been very few detailed studies on determining the contribution of grain-boundary sliding to creep in ceramics.

To date, there have been only six published reports on measurements of grain boundary sliding in ceramics [5, 37, 38, 44–46]. The grain-boundary sliding contributions may be determined directly by measuring offsets in marker lines on the specimen surface or from the displacements of adjacent grains perpendicular to the specimen surface. As noted earlier by Langdon [47], two of the previous studies on ceramics [45, 46] used an incorrect indirect technique which overestimated the grain-boundary sliding contribution. Wakai and Kato [5] also used an indirect procedure, which possibly led to an overestimation of

0022–2461/90 $03.00 + .12

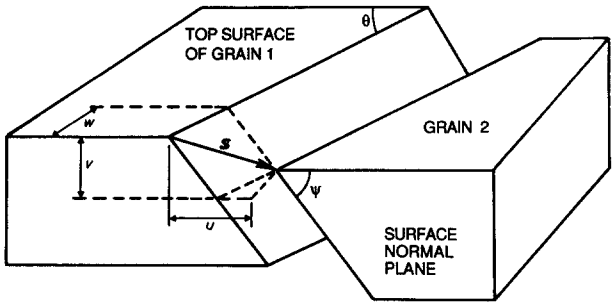

Figure 1 Schematic illustration of grain-boundary sliding. The strain due to grain-boundary sliding was calculated from measurements of the w component of the sliding vector **s**.

the grain boundary sliding contribution to creep. Heard and Raleigh [44] determined the sliding contribution from experiments under constant strain rate conditions, in contrast to the constant stress conditions utilized in other studies [37, 38, 45, 46]; also, they do not provide sufficient information on the procedures used to measure the sliding contribution so that it is not possible to evaluate their measurements critically. Consequently, currently there are only two acceptable reports on measurements of grain-boundary sliding: Langdon [37] and Cannon and Sherby [38] examined grain-boundary sliding during creep in compression. Clearly, it is desirable to obtain more quantitative information on the occurrence of grain boundary during creep in ceramics.

The present investigation was therefore undertaken with the following four specific objectives. First, to obtain quantitative information on the distribution of the magnitudes of grain boundary offsets during creep deformation. Second, to determine the grain-boundary sliding contribution to creep on the tensile surfaces of specimens creep tested in flexure. Third, to evaluate the prospects for superplasticity in structural ceramics on the basis of the present experimental results. Fourth, to examine the possible rate controlling mechanisms for creep in view of the present study.

2. Experimental procedure and materials

The experimental technique for determining the magnitude of the strain that can be attributed to grain boundary sliding is illustrated schematically in Fig. 1. The imposition of a tensile stress along the horizontal direction leads to grain boundary sliding, as shown in Fig. 1: **s** represents the sliding vector in the boundary plane. The sliding vector may be resolved into three mutually perpendicular components u, v and w; u is parallel to the tensile axis, v is perpendicular to both the tensile axis and surface plane, and w is perpendicular to the tensile axis but in the plane of the specimen surface. The strain due to grain boundary sliding may be calculated by measuring any one of these components and the associated angles shown in Fig. 1. It is difficult to measure the **u** component accurately and it is also quite tedious to make a large number of measurements of the angles. However, as shown by Langdon [48], the strain due to grain-boundary sliding, ε_{gbs}, may be determined reasonably by measuring the offsets w along several grain boundaries and using the following expression:

$$\varepsilon_{gbs} = \phi \bar{w}/\bar{L} \quad (1)$$

where ϕ is a constant (equal to 1.5), $\bar{w}$ is the average value of grain boundary offset, and $\bar{L}$ is the mean linear intercept grain size.

Polycrystalline alumina was chosen as the material for the present study. Two different samples of polycrystalline alumina were examined: one was a commercially hot-pressed alumina doped with 0.25% MgO used in a previous investigation [49] and the other was made with high purity alumina powder using a procedure described previously for making silicon carbide whisker reinforced alumina composites [50]. The commercial alumina had an initial linear intercept grain size, $\bar{L}$, of 0.92 μm [49], whereas the high purity alumina had a substantially larger grain size of 5.5 μm.

Creep specimens with nominal dimension of 3 mm × 3 mm were diamond machined using a low speed diamond saw. The tensile faces of the specimens were polished to a smooth scratch-free finish. Marker lines were then inscribed parallel to the tensile axis by rubbing a specimen surface once with a lens tissue saturated with alcohol and 3 μm diamond paste. The creep tests were conducted in four-point bending mode at a temperature of 1673 K, using an experimental set-up described earlier [49]. The tensile stresses and strains at the outer surface were calculated using a procedure described by Hollenberg *et al.* [51]. The tensile surfaces of creep tested specimens were examined by scanning electron microscopy. Photomicrographs were taken at magnifications of over 2000 × at more than 20 different locations. The negatives of these photomicrographs were placed on a light box and the offsets in marker lines were measured using an eye piece with 10 × magnification. Using this procedure, it was possible to measure sliding offsets of ~ 0.05 μm and larger. Offsets in marker lines were measured at over 250 different grain boundaries and ε_{gbs} was calculated using Equation 1.

3. Experimental results

3.1. Mechanical properties

The creep characteristics for the two specimens tested in this investigation are illustrated in Fig. 2 as a plot of strain rate, $\dot{\varepsilon}$, against strain. It is to be noted that d in Fig. 2 refers to the spatial grain size of the material and it is defined as $d = 1.74\bar{L}$. The specimens with spatial grain sizes of 1.6 and 9.5 μm were tested at stresses of 44 and 36 MPa, respectively.

Inspection of Fig. 2 reveals that both the specimens exhibit a primary creep region up to strains of $\sim 2\%$, where the strain rate is decreasing, and a well defined steady-state region at higher strains, where the strain rate is constant. In general, the elevated temperature mechanical properties of polycrystalline materials may be represented in the following form:

$$\dot{\varepsilon} = \frac{ADGb}{kT}\left(\frac{\mathbf{b}}{d}\right)^p\left(\frac{\sigma}{G}\right)^n \quad (2)$$

where A is a dimensionless constant, D is the appropriate diffusion coefficient, G is the shear modulus, **b**

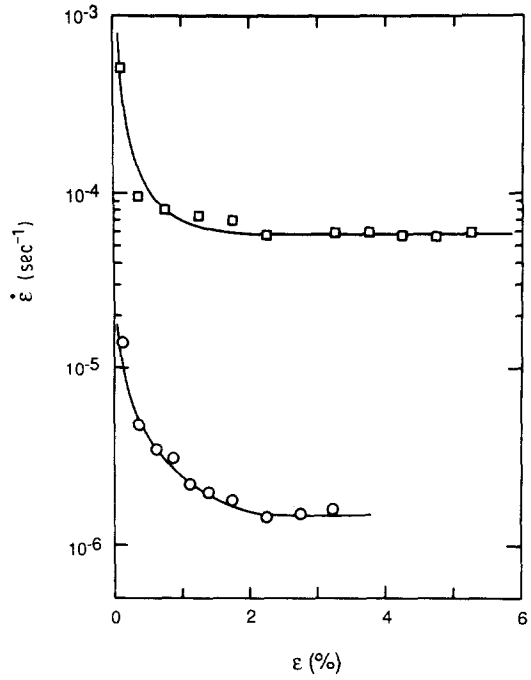

Figure 2 The variation in strain rate with strain for polycrystalline alumina with grain sizes of (□) 1.6 and (○) 9.5 μm of the specimens tested at stresses of 44 and 36 MPa, respectively. T = 1673 K.

is the magnitude of the Burger's vector, k is Boltzmann's constant, T is the absolute temperature and the exponents p and n are constants. It was shown earlier for the commercial polycrystalline alumina that $n = 2$ [49] and $p = 1.6$ [52]. Thus, the higher creep rate for the commercial alumina may be attributed to the lower grain size of this material and the higher stress imposed on this specimen.

3.2. Qualitative observations of grain-boundary sliding

Figures 3a and b show typical surface features in the commercially hot-pressed alumina specimen tested to a strain of 5.5% at a stress of 44 MPa. The tensile axis is horizontal. The occurrence of grain-boundary sliding during creep deformation, and crack formation, is clearly visible at the grain boundary marked A in Fig. 3a. The offsets in the marker lines were generally quite small. Also, inspection of Fig. 3b indicates that the grain labelled B is rotated with respect to the adjacent grains along the tensile axis.

Figures 4a and b illustrate the surface features in the high purity alumina specimen tested to a strain of 3.9% at a stress of 36 MPa. The tensile axis is horizontal. The offset in the marker line at the grain boundary marked E in Fig. 4a clearly reveals the occurrence of grain-boundary sliding, and an examination of Fig. 4b indicates that grain F is rotated with respect to the adjacent grains. A comparison of Fig. 4 with Fig. 3 reveals that the magnitudes of the sliding offsets were substantially smaller in the finer grained commercial alumina.

3.3. Quantitative measurements of grain-boundary sliding

The offsets in the marker lines in the fine-grained commercial alumina were very small and, therefore, it was not possible to make meaningful measurements of the grain-boundary sliding offsets on this specimen.

In contrast to the commercial alumina, the grain boundary offsets in the high purity alumina specimen very fairly large and these could be measured quite easily. The offsets in marker lines were recorded at over 250 grain boundaries and the experimental results are summarized in Fig. 5 in the form of a plot of the number of boundaries against the corresponding offset value, w, in increments of 0.1 μm. With the exception of two offset values of 0.6 μm, all sliding offsets were in the range of 0 to 0.3 μm. Inspection of Fig. 5 reveals that the most frequently occurring offset value is in the range of 0.1 to 0.2 μm.

An average offset value of $\bar{w} = 0.10 + 0.009\,\mu$m was determined from the experimental data shown in Fig. 5. Putting $\phi = 1.5$, $\bar{w} = 0.1\,\mu$m and $\bar{L} = 5.5\,\mu$m into Equation 1, the strain due to grain-boundary sliding, ε_{gbs}, is calculated to be 2.7%. Thus, noting that the total strain $\varepsilon = 3.9\%$, the grain-boundary sliding contribution to creep deformation, ξ (equal to $\varepsilon_{gbs}/\varepsilon$), is determined to be 70 $\pm$ 6.2%. It is important to note that the majority of the contribution (> 60%) to ε_{gbs} arises from offsets in the range of 0.1 to 0.2 μm.

4. Discussion

4.1. Mechanical properties

The creep characteristics of the commercial alumina were reported earlier [49, 52]: these studies showed that the stress exponent $n \simeq 2$ and that the inverse

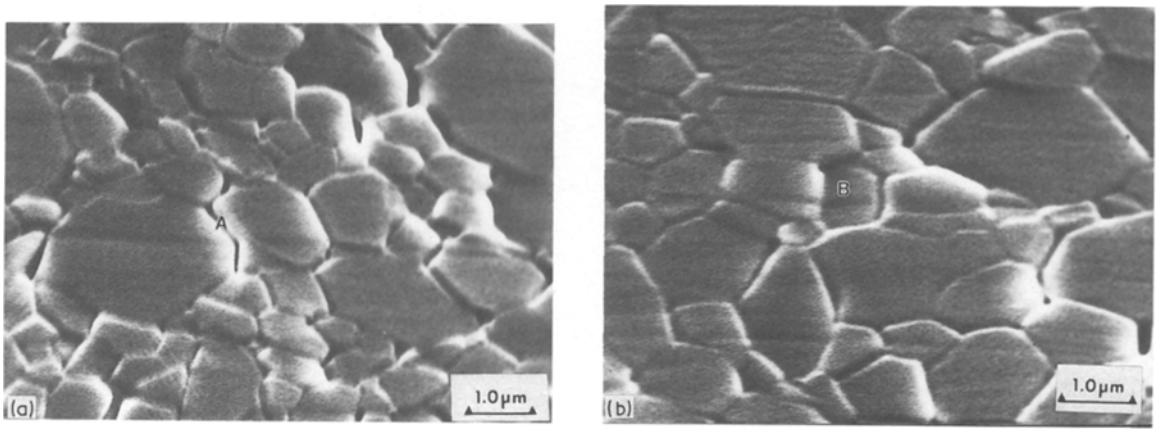

Figure 3 Scanning electron micrographs of the specimen with a grain size of 1.6 μm tested to a strain of 5.5% illustrating the occurrence of (a) grain-boundary sliding at A and (b) grain rotation at B. The tensile axis is horizontal.

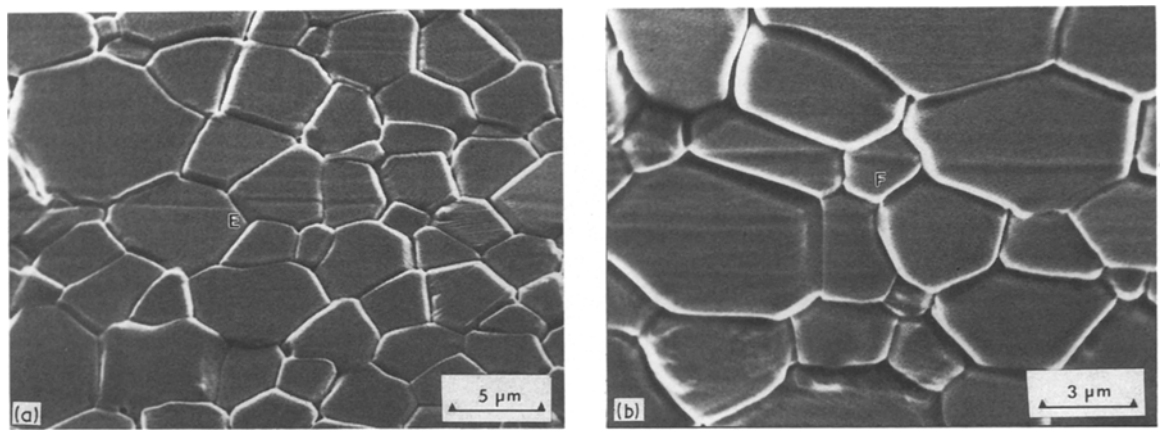

Figure 4 Scanning electron micrographs of the specimen with a grain size of 9.5 μm tested to a strain of 3.9% illustrating the occurrence of (a) grain-boundary sliding at E and (b) grain rotation at F. The tensile axis is horizontal.

grain size exponent $p = 1.6 \pm 0.2$. In the present investigation, the high purity alumina was examined primarily because of its larger grain size which, it was anticipated, would enable measurements of sliding to be accomplished fairly easily. It is important, however, to examine whether the larger grained alumina is deforming by the same mechanism as the commercial alumina studied previously.

Assuming that there is no change in the rate controlling creep mechanism, Equation 2 may be re-written as follows:

$$(d_1/d_2)^p = (\sigma_1/\sigma_2)^n (\dot{\varepsilon}_2/\dot{\varepsilon}_1) \quad (3)$$

where the subscripts 1 and 2 refer to the commercial and high purity alumina, respectively. The value of p in Equation 3 may be determined by assuming $n = 2$ and putting $\dot{\varepsilon}_1 = 5.8 \times 10^{-5}\,\text{sec}^{-1}$, $\dot{\varepsilon}_2 = 1.6 \times 10^{-6}\,\text{sec}^{-1}$, $\sigma_1 = 44\,\text{MPa}$, $\sigma_2 = 36\,\text{MPa}$, $d_1 = 1.6\,\mu\text{m}$ and $d_2 = 9.5\,\mu\text{m}$. The above calculation reveals that $p \simeq 1.8$. This value is in excellent agreement with the value of p ($= 1.6 \pm 0.2$) determined earlier for the commercial alumina, and this leads to the conclusion that the alumina with a grain size of 9.5 μm is deforming by the same mechanism as the alumina with a grain size of 1.6 μm. In the earlier investigation, it was suggested that the commercial alumina was deforming by an interface reaction controlled diffusion creep mechanism [49].

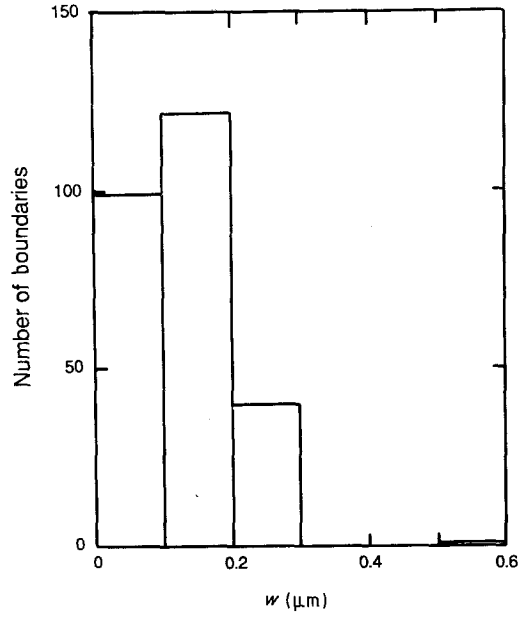

Figure 5 Number of boundaries against offset w. $T = 1673\,\text{K}$, $d = 9.5\,\mu\text{m}$, $\varepsilon = 3.9\%$.

4.2. Comparison with previous investigations

Clearly, it is necessary to establish that the present experimental measurements made at the specimen surface are representative of deformation in the interior of a specimen. In this context, it is to be noted that there have been three investigations of sliding in which measurements made in the interior of a specimen have been compared with those made at the surface [53–55]. In these investigations, grain-boundary sliding in the specimen interior was examined by measuring offsets at grain boundaries in stringers of oxides which acted as internal markers. All three investigations showed that ξ calculated from measurements at the surface is identical to that calculated from measurements in the interior of a specimen. Therefore, it is concluded that the present experimental measurements demonstrate that grain-boundary sliding is an important deformation mode during tensile creep in fine grained alumina.

All of the published measurements of grain-boundary sliding in ceramics are summarized in Table I. The various columns in Table I identify the experimental materials, testing procedures, techniques for measuring grain-boundary sliding, the grain-boundary sliding contribution to creep, ξ, and the references, respectively. Wakai and Kato [5], Hensler and Cullen [45] and Tokar [46] determined ε_{gbs} using an indirect technique which assumed that $\varepsilon = \varepsilon_g + \varepsilon_{gbs}$, where ε_g is the strain due to intragranular deformation. The value of ε_g was determined from measurements of the elongation of grains, but as noted by Langdon [47] and demonstrated by Cannon and Sherby [38] there is tendency for boundaries to migrate during creep to maintain an equiaxed grain shape. Thus, the value of ε_g is underestimated and, consequently, the value of ε_{gbs} is overestimated by this indirect technique. Heard and Raleigh [44] reported measurements of sliding during constant strain rate experiments, but they do not provide sufficient information to evaluate their measurements critically. Cannon and Sherby [38] and

TABLE I Measurements of grain-boundary sliding in ceramics

Material	Testing conditions	Method	ξ (%)	Reference
ZrO_2	Tension	Indirect*	$\simeq$ 60–80	Wakai and Kato [5]
MgO	Compression	Indirect*	100	Hensler and Cullen [45]
$CaCO_3$	Compression with superimposed hydrostatic pressure	Offset (w)	10–20	Heard and Raleigh [44]
$U_{0.79}Pu_{0.21}C_{1.02}$	Compression	Indirect*	80–100	Tokar [46]
MgO	Compression	Offset (v)	4–20	Langdon [37]
Al_2O_3	Compression	Offset (v)	40–56	Cannon and Sherby [38]
Al_2O_3	Bending (tensile surface)	Offset (w)	70	Present study

*assumes $\varepsilon = \varepsilon_g + \varepsilon_{gbs}$

Langdon [37] measured grain-boundary sliding during compression creep in alumina and magnesia, respectively, from measurements of the vertical components of sliding, v in Fig. 1. Both these studies showed that the sliding contribution to creep increases with a decrease in the grain size and Langdon [37] demonstrated also that ξ increases with a decrease in stress. Cannon and Sherby [38] reported average values of ξ at a stress of $\sim$83 MPa to be $\sim$58 and 44% for specimens tested with grain sizes of $\sim$20 to 30 μm and $\sim$65 μm, respectively. The present experimental measurement of ξ on the tensile surface of creep tested alumina is consistent with those of Cannon and Sherby, when it is noted that the present study utilized material with a linear intercept grain size of 5.5 μm and a stress of 36 MPa.

4.3. Prospects for superplasticity

Superplasticity refers to the ability of some polycrystalline materials to exhibit extremely large strains to failure. This phenomenon may be utilized to form complex shapes, and it is being used currently to manufacture metallic components for aerospace applications. There is increasing interest in examining superplasticity in structural ceramics with a view to using this phenomenon for forming ceramic components [1–6]. It is now well established that, in metallic superplastic alloys, the grain-boundary sliding contribution to deformation is greater than $\sim$50% under optimum superplastic conditions [25]. Based on the present experimental measurements, it is of interest to examine the possibility for superplasticity in polycrystalline alumina.

Table II presents in a comparative format some important characteristics of superplastic deformation in metallic alloys and creep deformation in polycrystalline alumina. It is clear from an inspection of Table II that deformation in polycrystalline alumina, like superplastic metallic alloys, is associated with a stress exponent n of $\sim$2 and a similar range in values of the inverse grain size exponent p. The present experimental measurements demonstrate also that, like superplastic alloys, polycrystalline alumina exhibits extensive grain-boundary sliding. On the basis of this comparison, it is reasonable to anticipate that polycrystalline alumina may behave in a superplastic manner, and this has been demonstrated in compression in a few recent studies [1, 3, 56–58].

TABLE II Comparison of the characteristics of superplastic alloys with polycrystalline alumina

Parameter	Superplastic alloys	Alumina
Stress exponent (n)	$\lesssim$2	$\simeq$2
Inverse grain size exponent (p)	$\simeq$2–3	$\simeq$1.5–2.5
Grain boundary sliding contribution (ξ)	$\gtrsim$50%	70 $\pm$ 6.2%

One of the major limitations to attaining large tensile strains prior to failure is the nucleation and growth of cavities during creep in alumina [3, 7, 9, 11, 14, 16, 20, 32, 57]. However, it is important to note that, in contrast to metallic superplastic alloys where levels of cavitation at elongations to failure of $\sim$500% may attain values as high as 30%, the total volume fraction of cavitation in polycrystalline alumina is not very large: thus, Carry and Mocellin [57] reported a decrease in density in polycrystalline alumina by about 3 to 5% at strains of $\sim$50%. On the basis of this observation, it is anticipated that polycrystalline alumina may exhibit elongations to failure exceeding 100% under optimum experimental conditions. In this context, it is to be noted that Evans *et al.* [18] analysed cavity nucleation at grain boundary triple junctions, and they recommended procedures, in terms of experimental materials and conditions, to preclude cavity formation and promote superplasticity in ceramics.

Yttria stabilized tetragonal zirconia is a promising material for structural applications. It has been demonstrated that this material behaves in a superplastic-like manner under some experimental conditions [2, 4, 6]. Recently, Hermannson *et al.* [59] examined superplasticity in polycrystalline zirconia with a fine grain size of $\sim$0.25 μm. They used an indirect procedure to determine ε_{gbs}: $\varepsilon = \varepsilon_g + \varepsilon_{gbs} + \varepsilon_{cav}$, where ε_{cav} is the strain arising from cavitation during deformation. Subtracting the cavitation strain and the grain strain, ε_g, as determined from the elongation of the grains parallel to the tensile axis, they determined that $\xi > 80\%$ under superplastic conditions [59]. However, it is important to emphasize the determinations of grain strain from measurements of grain elongation tend to underestimate ε_g and overestimate ξ.

4.4. Implications for rate controlling creep mechanisms

There have been numerous studies on creep in fine grained alumina, and many different explanations have been put forward to rationalize the experimental results. The present experimental study may provide an important insight into the rate controlling deformation mechanism: thus, any reasonable rate controlling mechanism suggested should be able to account for the large contribution of grain boundary sliding to creep. The following three rate controlling mechanisms are discussed in the subsequent sections: (a) diffusion creep, (b) deformation in the region of transition from diffusion to dislocation power-law creep, and (c) grain-boundary sliding and interface controlled diffusion creep.

4.4.1. The possibility of deformation by diffusion creep

Transmission electron microscopy studies of fine grained alumina indicate that there is very little intragranular dislocation activity during creep deformation [7, 17, 20, 32] and, consequently, creep in fine grained alumina is usually attributed to some form of diffusion creep. Diffusion creep involves the movement of vacancies either through the matrix or along grain boundaries: these processes are referred to as Nabarro-Herring [60, 61] and Coble [62] creep mechanisms, respectively. Diffusion creep in ceramics was examined recently on the basis of deformation mechanism maps, and the behaviour of ceramics was compared with those of metals [63]. As noted originally by Lifshitz [64], in order to maintain specimen coherency, grain-boundary sliding is a necessary component of diffusion creep. Depending upon the geometry and the procedures adopted, the grain boundary sliding contribution to diffusion creep is estimated to be greater than $\sim 50\%$ [38].

It is important to note that the occurrence of grain-boundary sliding, as a part of diffusion creep, would lead to offsets in the marker lines similar to those arising from the occurrence of grain-boundary sliding as an independent deformation mechanism. However, although there have been a few studies on fine grained alumina showing that $n \simeq 1$ [38, 58], most studies have reported values of n in the range of 1.5 to 2 [7, 17, 19, 20, 32, 49]. The experimental observation of $n \simeq 2$ is in contrast to the $n = 1$ predicted by the diffusion creep theories [60–62]. Consequently, the present results cannot be attributed directly to a diffusion creep mechanism.

4.4.2. Deformation in the region of transition from diffusion to dislocation power law creep

In general, creep at elevated temperatures may occur by diffusion of vacancies from grain boundaries under tension to those under compression or by the intragranular movement of dislocations. Intragranular dislocation creep is frequently referred to power law creep because the creep rate may be expressed as $\dot{\varepsilon} \propto \sigma^n$, where the value of the exponent n is typically greater than ~ 3. Diffusion and power law creep operate independently so that creep is controlled by the mechanism giving rise to a higher strain rate. In ceramics with fine grain sizes, diffusion creep is dominant at low stresses and power law creep is dominant at high stresses. For alumina, the diffusion and power law creep mechanisms are associated with $n = 1$ and $n = 3$, respectively [38, 65].

A possible explanation for the experimentally observed stress exponent of $n = 2$ in fine grained alumina is that the data were obtained in the region of transition from diffusion to power law creep [66]. In this situation, it is possible that diffusion creep may lead to substantial grain boundary sliding. This possibility may be evaluated critically by comparing the experimental range of stresses used in the investigation with the theoretically predicted stress for the transition from diffusion to power law creep. By equating the strain rates due to the two mechanisms, Cannon and Langdon [65] determined the following expression for the stress for transition from diffusion to power law creep:

$$\sigma/G = 6.5(\mathbf{b}/d)(D_c/D_a)^{0.5} \quad (4)$$

where D_c and D_a are the coefficients for cation and anion diffusion through the lattice, respectively. It is important to note that Equation 4 assumes that diffusion creep is controlled by lattice cation diffusion and that power law creep is controlled by lattice anion diffusion. Putting in the lattice cation [67] and anion [68] diffusion coefficients in to Equation 4, and $\mathbf{b} = 0.475$ nm, the normalized transition stress is calculated to be $\sim 1.2 \times 10^{-2}$ for alumina with $d = 9.5\,\mu$m and $\sim 7.0 \times 10^{-2}$ for alumina with $d = 1.6\,\mu$m.

The previous investigation on commercial alumina [49] as well as the present one used stresses less than 100 MPa. Thus, noting that the value of the shear modulus at 1673 K is 1.3×10^5 MPa [49], the experiments were conducted at normalized stresses of $< 7.7 \times 10^{-4}$, which are two orders of magnitude smaller than the transition stress calculated above. The transition from diffusion to power-law creep is expected to be fairly sharp and, consequently, the experimental observations of $n \simeq 2$ cannot be attributed to data being obtained in the region of transition from diffusion to power-law creep.

4.4.3. Mechanisms based on grain-boundary sliding and interface controlled diffusion creep

Three different models have been developed, which consider grain-boundary sliding as an independent deformation mechanism [69–71], and they give expressions for the strain rate due to grain boundary sliding of the form of Equation 2, with the corresponding exponents n and p. It is not possible to compare these models with the experimental data obtained because the exponents n and p for grain-boundary sliding were not determined explicitly in the present study. However, it is to be noted that these models assume that grain-boundary sliding will be accommodated by processes such as the development of triple point cavities and cracks [69], the formation of triple point folds [70] and intragranular plastic

deformation [71]. There is very little evidence for the formation of triple point folds or substantial intragranular plastic deformation in fine grained alumina, so that these models are not directly applicable to alumina. The formation of triple point cavities has been reported in polycrystalline alumina, but it is not clear whether the observed cavitation at a limited number of triple points can completely accommodate the extensive grain boundary sliding occurring in fine grained alumina.

The standard theories for diffusion creep assume that grain boundaries act as perfect sources and sinks for vacancies [60–62]. If grain boundaries do not behave perfectly, then the formation or annihilation of vacancies may become the rate controlling step: this is referred to as interface controlled diffusion creep. It is clear that, since the formation, diffusion and annihilation of vacancies operate sequentially, the strain rate will be controlled by the slowest process. Thus, the creep rates by an interface controlled mechanism will be slower than those given by a standard diffusion mechanism. Since an interface controlled mechanism essentially involves the same process as the standard diffusion mechanism, it is anticipated that the interface mechanism would also give rise to substantial grain-boundary sliding.

Cannon *et al.* [72] reported a change in stress exponent from $n = 1$ to $n = 2$ with a decrease in stress. Such a transition would be consistent with the occurrence of an interface controlled diffusion mechanism at low stresses. However, it is necessary to confirm this explanation by showing that the interface controlled creep rates are slower than those given by the standard diffusion theories. Unfortunately, data on diffusion coefficients in polcrystalline alumina are sparse, especially since it was demonstrated recently that it is not reasonable to use diffusion data inferred from an analysis of experimental creep results [73]. Consequently, it is not possible to unambiguously identify interface control as the rate controlling creep mechanism. Also, it is important to note that, while theories for interface control predict an $n = 2$, they also predict $p = 1$ [74–77], which is in contrast to the typical values of $p \simeq 2$ in fine grained alumina.

Finally, it is noted that interface control has been suggested as a possible rate controlling mechanism for superplastic deformation [77, 78] in metallic alloys, and Wakai and Nagono [79] recently extended this concept to superplastic deformation in polycrystalline yttria stabilized zirconia.

5. Summary and conclusion

1. There is considerable evidence for the occurrence of grain-boundary sliding and grain rotation during creep in polycrystalline alumina.

2. Experimental measurements of the offsets in marker lines at grain boundaries reveal that the grain-boundary sliding contribution to creep strain is $70 \pm 6.2\%$.

3. Based on the large contribution of grain-boundary sliding, and a comparison with the other mechanical properties of metallic superplastic alloys, it is concluded that polycrystalline alumina exhibits superplastic characteristics.

4. A critical examination of several possible rate controlling creep mechanisms indicates that creep occurs by either an independent grain-boundary sliding mechanism or an interface controlled diffusion creep mechanism.

Acknowledgements

The author is grateful to Dr John R. Porter of Rockwell International Science center for providing the material used in this study. The experimental creep study was conducted at the University of Southern California with support from the National Science Foundation under Grant No. DMR 8217120. He also acknowledges with gratitude the encouragement and support provided by Professor A. K. Mukherjee of the University of California at Davis. This work was supported in part by the Center of Excellence for Advanced Materials, established at the University of California, San Diego, by the US Army research office, and by the US Army Research Office under contract No. DAAL03-89-K-0145.

References

1. C. CARRY and A. MOCELLIN, in "Superplasticity", edited by B. Baudelet and M. Suery (Centre National de la Recherche Scientifique, Paris, 1985) p. 16.1.
2. F. WAKAI, S. SAKAGUCHI and Y. MATSUNO, *Adv. Ceram. Mater.* **1** (1986) 259.
3. C. CARRY and A. MOCELLIN, in "High Tech Ceramics", edited by P. Vincenzini (Elsevier, Amsterdam, 1987) p. 1043.
4. R. DUCLOS and J. CRAMPON, *J. Mater. Sci. Lett.* **6** (1987) 905.
5. R. WAKAI and H. KATO, *Adv. Ceram. Mater.* **3** (1988) 71.
6. T. G. NIEH, C. M. McNALLY and J. WADSWORTH, *Scripta Metall.* **22** (1988) 1297.
7. J. R. PORTER, W. BLUMENTHAL and A. G. EVANS, *Acta Metall.* **29** (1981) 1899.
8. C. H. HSUEH and A. G. EVANS, *ibid.* **29** (1981) 1907.
9. A. G. EVANS, in "Recent Advances in Creep and Fracture of Engineering Materials and Structures", edited by B. Wilshire and D. R. G. Owen (Pineridge Press, Swansea, 1982) p. 53.
10. R. L. TSAI and R. RAJ, *Acta Metall.* **30** (1982) 1043.
11. R. A. PAGE, J. LANKFORD and S. SPOONER, *J. Mater. Sci.* **19** (1984) 3360.
12. K. S. CHAN, J. LANKFORD and R. A. PAGE, *Acta Metall.* **32** (1984) 1907.
13. S. M. WIEDERHORN, L. CHUCK, E. R. FULLER and N. J. TIGHE, in "Tailoring Multiphase and Composite Ceramics", edited by R. E. Tressler, G. L. Messing, C. G. Pantano and R. E. Newnham (Plenum, New York, 1986) p. 755.
14. K. JAKUS, S. M. WIEDERHORN and B. J. HOCKEY, *J. Amer. Ceram. Soc.* **69** (1986) 725.
15. K. S. CHAN, R. A. PAGE and J. LANKFORD, *Acta Metall.* **34** (1986) 2361.
16. A. H. CHOKSHI and J. R. PORTER, *J. Amer. Ceram. Soc.* **70** (1987) 197.
17. A. H. HEUER, R. M. CANNON and N. J. TIGHE, in "Ultrafine-Grain Ceramics", edited by J. J. Burke, N. L. Reed and V. Weiss (Syracuse University Press, Syracuse, New York, 1970) p. 339.
18. A. G. EVANS, J. R. RICE and J. P. HIRTH, *J. Amer. Ceram. Soc.* **63** (1980) 368.
19. T. SUGITA and J. A. PASK, *ibid.* **53** (1970) 609.
20. R. S. JUPP and B. J. PLETKA, in "Deformation of

Ceramic Materials II", edited by R. E. Tressler and R. C. Bradt (Plenum Press, New York, 1984) p. 405.
21. R. N. STEVENS, *Metall. Rev.* **11** (1966) 129.
22. R. L. BELL and T. G. LANGDON, in "Interfaces", edited by R. C. Gifkins (Butterworths, Australia, 1969) p. 115.
23. H. GLEITER and B. CHALMERS, *Prog. Mater. Sci.* **16** (1972) 1.
24. T. G. LANGDON and R. B. VASTAVA, in "Mechanical Testing for Deformation Model Development", edited by R. W. Rohde and J. C. Swearengen (American Society for Testing and Materials, Philadelphia, PA, 1982) p. 435.
25. Z.-R. LIN, A. H. CHOKSHI and T. G. LANGDON, *J. Mater. Sci.* **23** (1988) 2712.
26. F. F. LANGE, D. R. CLARKE and B. I. DAVIS, *ibid.* **15** (1980) 611.
27. R. CHANG, *J. Nucl. Mater.* **2** (1959) 174.
28. D. R. MOSHER, R. RAJ and R. KOSSOWSKY, *J. Mater. Sci.* **11** (1976) 49.
29. R. L. TSAI and R. RAJ, *J. Amer. Ceram. Soc.* **63** (1980) 513.
30. M. A. ADAMS and G. T. MURRAY, *J. App. Phys.* **33** (1962) 2126.
31. P. F. BECHER and H. PALMOUR III, *J. Amer. Ceram. Soc.* **53** (1970) 119.
32. A. H. HEUER, N. J. TIGHE and R. M. CANNON, *ibid.* **63** (1980) 53.
33. S. WHITE, *Nature Phy. Sci.* **234** (1971) 175.
34. W. J. BRINDLEY and B. J. PLETKA, in "Deformation of Ceramic Materials II", edited by R. E. Tressler and R. C. Bradt (Plenum Press, New York, 1984) p. 417.
35. P. M. BURKE, PhD thesis, Stanford University, 1968.
36. T. G. LANGDON and J. A. PASK, *J. Amer. Ceram. Soc.* **54** (1971) 240.
37. T. G. LANGDON, *ibid.* **58** (1975) 92.
38. W. R. CANNON and O. D. SHERBY, *ibid.* **60** (1977) 44.
39. W. M. ARMSTRONG and W. R. IRVINE, *J. Nucl. Mater.* **9** (1963) 121.
40. *Idem, ibid.* **12** (1964) 261.
41. S. M. COPLEY and J. A. PASK, *J. Amer. Ceram. Soc.* **48** (1965) 636.
42. L. E. POTEAT and C. S. YUST, *ibid.* **49** (1966) 410.
43. W. R. CANNON, PhD thesis, Stanford University, 1971.
44. H. C. HEARD and C. B. RALEIGH, *Geol. Soc. Amer. Bull.* **83** (1972) 935.
45. J. H. HENSLAR and G. V. CULLEN, *J. Amer. Ceram. Soc.* **50** (1967) 584.
46. M. TOKAR, *ibid.* **56** (1973) 173.
47. T. G. LANGDON, in "Deformation of Ceramic Materials" (Plenum, New York, 1975) p. 101.
48. T. G. LANGDON, *Metall. Trans.* **3** (1972) 797.
49. A. H. CHOKSHI and J. R. PORTER, *J. Mater. Sci.* **21** (1986) 705.
50. J. R. PORTER, F. F. LANGE and A. H. CHOKSHI, *Ceram. Bull.* **66** (1987) 343.
51. G. W. HOLLENBERG, G. R. TERWILLINGER and R. S. GORDON, *J. Amer. Ceram. Soc.* **54** (1971) 196.
52. A. H. CHOKSHI and J. R. PORTER, *ibid.* **69** (1986) C37.
53. Y. ISHIDA, A. W. MULLENDORE and N. J. GRANT, *Trans. AIME* **233** (1965) 204.
54. R. L. BELL and C. GRAEME-BARBER, *J. Mater. Sci.* **5** (1970) 933.
55. K. MATSUKI, H. MORITA, Y. YAMADA and Y. MURAKAMI, *Metal Sci.* **11** (1977) 156.
56. W. R. CANNON, in "Structure and Properties of MgO and Al_2O_3 Ceramics", edited by W. D. Kingery (American Ceramic Society, Columbus, Ohio, 1985) p. 741.
57. C. CARRY and A. MOCELLIN, *Ceram. Inter.* **13** (1987) 89.
58. K. R. VENKATACHARI and R. RAJ, *J. Amer. Ceram. Soc.* **69** (1986) 135.
59. T. HERMANNSON, P. LANGERLOF and G. L. DUNLOP, in Superplasticity and Superplastic Forming edited by C. H. Hamilton and N. E. Paton (The Minerals, Metals and Materials Society, PA, 1988) p. 631.
60. F. R. N. NABARRO, in "Report on a Conference on Strength of Solids" (The Physical Society, London, 1948) p. 75.
61. C. HERRING, *J. App. Phys.* **21** (1950) 437.
62. R. L. COBLE, *ibid.* **34** (1963) 1679.
63. A. H. CHOKSHI and T. G. LANGDON, *Defect and Diffusion Forum* **66–69** (1989) 1205.
64. I. M. LIFSHITZ, *Soviet Phys. JETP* **17** (1963) 909.
65. W. R. CANNON and T. G. LANGDON, *J. Mater. Sci.* **23** (1988) 1.
66. C. K. L. DAVIES and K. S. RAY, in "Special Ceramics 5" edited by P. Popper (The British Ceramic Research Association, Stoke-on Trent, 1972) p. 193.
67. A. E. PALADINO and W. D. KINGERY, *J. Chem. Phys.* **37** (1962) 957.
68. Y. OISHI and W. D. KINGERY, *ibid.* **33** (1960) 480.
69. T. G. LANGDON, *Philos. Mag.* **22** (1970) 689.
70. R. C. GIFKINS, *J. Australian Inst. Metals* **18** (1973) 137.
71. F. W. CROSSMAN and M. F. ASHBY, *Acta Metall.* **23** (1975) 425.
72. R. M. CANNON, W. H. RHODES and A. H. HEUER, *J. Amer. Ceram. Soc.* **63** (1980) 46.
73. A. H. CHOKSHI, *ibid.* **71** (1988) C241.
74. M. F. ASHBY, *Scripta Metall.* **3** (1969) 837.
75. G. W. GREENWOOD, *ibid.* **4** (1970) 171.
76. B. BURTON, *Mater. Sci. Engng.* **10** (1972) 9.
77. M. F. ASHBY and R. A. VERRALL, *Acta Metall.* **21** (1973) 149.
78. J. H. SCHNEIBEL and P. M. HAZZLEDINE, *J. Mater. Sci.* **18** (1983) 562.
79. F. WAKAI and T. NAGONO, *J. Mater. Sci. Lett.* **7** (1988) 607.

Received 13 March
and accepted 30 August 1989